

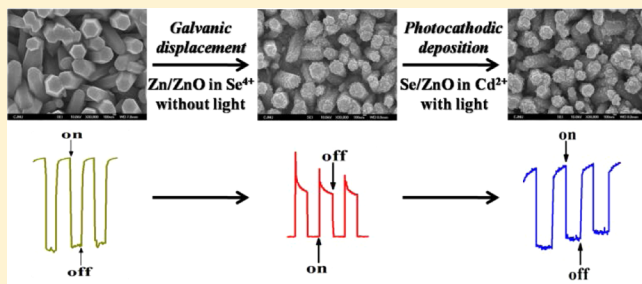
CdSe/ZnO Composite via Galvanic Displacement Followed by Photocathodic Deposition: Hybrid Electrosynthesis and Characterization

Seungun Choi,[†] Yujin Chae,[†] Sunyoung Ham,^{†,§} Wooju Lee,[†] Noseung Myung,^{*,†} and Krishnan Rajeshwar^{*,‡}

[†]Department of Applied Chemistry, Konkuk University, Chungju, Chungbuk 380-701, Republic of Korea

[‡]Department of Chemistry and Biochemistry, University of Texas at Arlington, Arlington, Texas 76019, United States

ABSTRACT: This study focuses on the preparation of CdSe/ZnO composite by combining three techniques, namely, electrodeposition, galvanic displacement, and photocathodic deposition. Thus ZnO nanowire array was first electrodeposited on Sn-doped indium oxide (ITO) or polycrystalline Au electrode; then, the metallic zinc codeposited with ZnO was galvanically replaced with Se from a Se⁴⁺ containing aqueous solution, which resulted in a Se/ZnO composite nanowire array. Finally, the Se component in Se/ZnO was photoelectrochemically reduced to Se²⁻ by irradiation. The Se species reacted with Cd²⁺ in the electrolyte phase to produce CdSe/ZnO composite in situ. The deposition details were elucidated in situ by a combination of stripping voltammetry and electrochemical quartz crystal microgravimetry. The composite sample was subsequently characterized by scanning electron microscopy, X-ray powder diffraction, energy-dispersive X-ray analyses, and photoelectrochemical (PEC) measurements. The PEC experiments revealed that the electrodeposited ZnO nanowire array behaved as an n-type semiconductor, which changed to p-type after deposition of Se. The ZnO/CdSe composite showed anodic photocurrents upon light illumination, again consistent with the n-type nature of both the composite components.



1. INTRODUCTION

Zinc oxide (ZnO), a wide band gap semiconductor ($E_g = \sim 3.4$ eV), has been intensely studied in recent years. Nanostructured 1-D morphologies of this material (e.g., array of nanotubes)^{2,3} are of both fundamental and practical interest because of the possibility of orthogonalizing electron collection and transport. Whereas the large band gap facilitates its use as a window material in photovoltaic devices, this attribute becomes a handicap in applications involving initial absorption of the solar spectrum or visible light. Spectral sensitization with dyes and semiconductor nanoparticles are two important approaches to circumventing this handicap.^{4–6} However, as discussed by a previous author,⁷ sensitization with another (lower band gap) semiconductor offers several advantages over dye sensitization, including, for example, potentially higher optical absorption, greater chemical and photostability, and the possibility of tailoring the band gap of the semiconductor sensitizer via the size quantization effect. This study describes an approach for preparing CdSe/ZnO using a combination of three techniques: electrodeposition, galvanic displacement, and photocathodic deposition.

Whereas sensitization of TiO₂ to encompass the visible range of the electromagnetic spectrum has been extensively investigated, much less effort has been devoted to the sensitization of ZnO with narrow band gap semiconductors.

Quantum dots of CdS or CdSe have been attached to ZnO nanospheres^{8,9} and nanorods.^{5,6} Quantum dots have been coated on ZnO nanorods by chemical bath deposition.^{4,10} Several reports have demonstrated^{11–13} that CdSe can be coated on ZnO nanowires and nanotubes by electrodeposition. It is worth noting that electrodeposition is a thermally mild, cost-effective, simple, and versatile method for the preparation of semiconductor thin films.^{14–16}

An innovative aspect of this study is a hybrid scheme combining electrodeposition with two other film deposition techniques, namely, galvanic displacement and photocathodic deposition. Galvanic displacement is a versatile, facile, and efficient interfacial technique that requires no external stimulus to proceed. Instead, an electrochemical potential gradient between a substrate and solution-borne ionic precursor leads to a spontaneous redox reaction resulting in film deposition.^{17–20} The light-absorption property of a semiconductor substrate may be exploited for photodepositing another semiconductor on top of it, as demonstrated by us for Se/TiO₂, CdSe/TiO₂, and PbSe/TiO₂.^{21,22} In this approach, the important point to note is that the Se initially photodeposited on the oxide surface

Received: May 2, 2012

Revised: August 8, 2012

Published: September 4, 2012

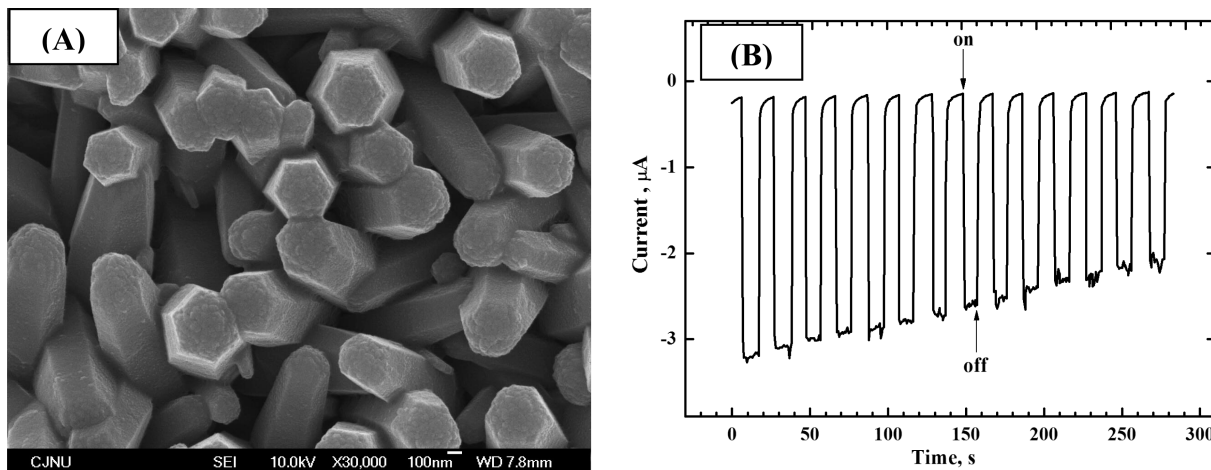


Figure 1. (A) SEM image of a ZnO nanowire array electrodeposited on ITO at -1.15 V and $70\text{ }^\circ\text{C}$ for 2000 s in 0.1 M KNO_3 containing 10 mM $\text{Zn}(\text{NO}_3)_2$. (B) Photocurrent transients in 0.1 M KNO_3 supporting electrolyte at a fixed bias potential of 0.50 V .

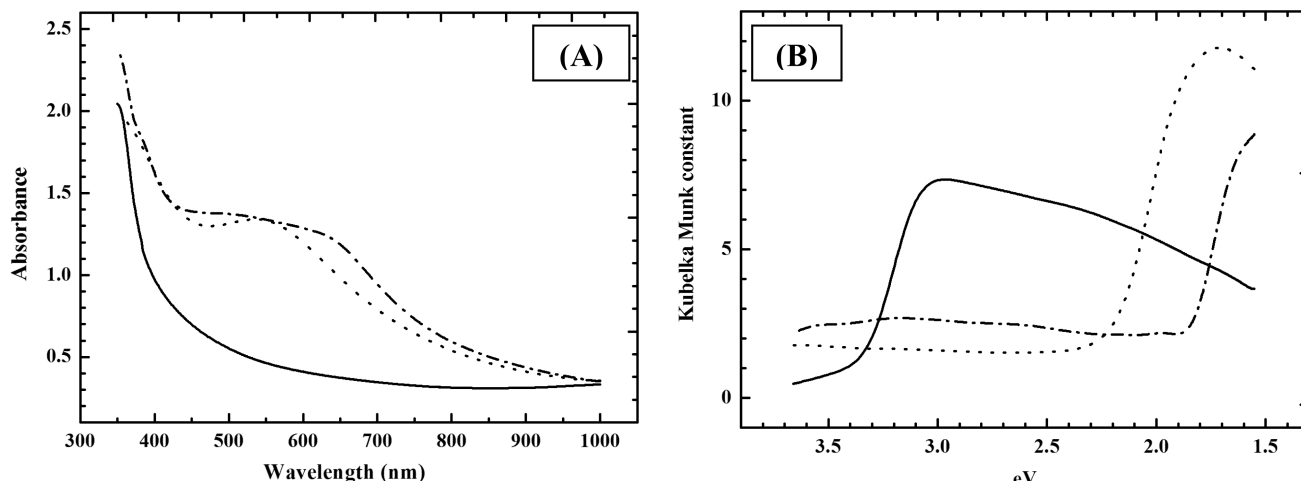


Figure 2. Absorption spectra (A) and diffuse reflectance spectra (B) of ZnO nanorod array (—), Se/ZnO (—●—●—), and CdSe/ZnO (---). The latter data are expressed in terms of the Kubelka–Munk formalism. ZnO was electrodeposited on ITO at -1.15 V for 1200 s using a 0.1 M KNO_3 containing 10 mM of $\text{Zn}(\text{NO}_3)_2$ at $70\text{ }^\circ\text{C}$. Se/ZnO was prepared by a galvanic replacement reaction in a 50 mM SeO_2 solution for 300 s . CdSe/ZnO was prepared by a hybrid sequence of electrodeposition, galvanic replacement, and photoinduced cathodic deposition in 0.1 M KNO_3 containing 20 mM CdSO_4 at the potential of -0.30 V for 300 s .

drives the subsequent underpotential deposition of Cd and Pb, leading to compound (CdSe and PbSe) formation. In the absence of Se, Cd, and Pb, photodeposition would not have occurred because of their relatively negative redox potentials relative to the TiO_2 conduction band edge.^{21,22}

We demonstrate the hybrid scheme with the electrosynthesis of CdSe/ZnO as a representative example. Heterojunctions of CdSe/ZnO are of importance in a wide array of optoelectronic applications, including photovoltaic solar conversion devices.^{5–9}

Finally, it is important to differentiate the hybrid scheme developed here with previous electrodeposition studies on CdSe/ZnO composites.^{2,3,11–13,23} The additional use of light in an electrodeposition scheme, as employed in the present study and in previous studies from our laboratories,^{21,22,24} immediately opens up the possibility of spatially defining areas for electrodeposition to occur and for developing patterns via the use of suitable masks.²³ A reviewer also pointed out another approach for transforming an oxide surface to a chalcogenide composition involving two consecutive ion exchange steps in the gas phase and in solution.²⁵ To our knowledge, this method

was not used for preparing CdSe/ZnO; nonetheless, it is worth noting that this strategy of “nanostructure transfer”²⁵ involves the use of toxic chemicals in the gas phase (such as H_2S) or the use of elevated temperatures for the chemical transformation unlike the mild conditions used in the present study.

2. EXPERIMENTAL SECTION

Electrodeposition of the ZnO nanowire array was performed in a conventional three-electrode electrochemical cell consisting of Sn-doped indium oxide (ITO) working electrode, Ag/AgCl/3 M NaCl reference electrode, and Pt wire or foil counter-electrode. The ITO working electrode was sonicated in a mixture of ethanol/ H_2O (1:3) and acetone/ H_2O (1:3) for 20 min, respectively, and finally rinsed with distilled water prior to use.²⁶ For all electrodeposition experiments, a μ Autolab Type III potentiostat/galvanostat (Eco Chemie, Netherlands) was used, and the temperature of the electrolyte was maintained at $70\text{ }^\circ\text{C}$ using a water bath. An EG&G Princeton Applied Research (PAR) 263A potentiostat/galvanostat equipped with model M250/270 electrochemistry software was used for

photoelectrochemical experiments and a Seiko EG&G model QCA 917 instrument consisting of an oscillator module (QCA 917-11), a 9 MHz AT-cut Au-coated quartz crystal (geometric area, 0.2 cm^2) working electrode, a Pt counterelectrode, and a Ag/AgCl/3 M NaCl reference electrode were used for electrochemical quartz crystal microgravimetry (EQCM). Details of the electrochemical instrumentation and the EQCM setup along with its calibration are given elsewhere.²⁷ All potentials below are quoted with respect to the Ag/AgCl/3 M NaCl reference electrode. In some cases, the electrodeposited ZnO nanowire array was annealed at 250°C for 1 h in air using a furnace.

The deposited films were irradiated with a 300 W xenon arc lamp contained in a Muller Elektronik-Optik LAX 1530 housing and connected to a Muller Elektronik-Optik SVX 1530 power source. A cutoff optical filter ($\sim 420 \text{ nm}$) (Edmund Optic) was used as needed. The incident light intensity on the electrode surface, as measured with a Newport model 70260 radiant power meter/model 70268 probe, was $\sim 100 \text{ mW/cm}^2$ in all experiments described below. The exposed area of the ITO surface was 0.2 cm^2 . Film morphology and composition were obtained on a field emission scanning electron microscope (JEOL model 6700F) equipped with an energy-dispersive X-ray analysis (EDX) probe. X-ray diffraction (XRD) patterns were recorded on a Bruker D8 Advance diffractometer with a Cu $\text{K}\alpha$ radiation source. The diffuse reflectance of the deposited films was measured at room temperature with a Perkin-Elmer Lamda 25 UV-vis spectrometer equipped with an integrating sphere (Labsphere RSA-PE-20).

All chemicals including zinc nitrate, potassium nitrate, cadmium sulfate hydrate, selenium dioxide, and sodium sulfate were from Aldrich and used without further purification. All procedures described below (except thermal anneal) were performed at the laboratory ambient temperature ($25 \pm 2^\circ\text{C}$).

3. RESULTS AND DISCUSSION

3.1. Electrodeposition of Zn/ZnO Nanowire Array.

Figure 1A shows an SEM image of the ZnO nanowire array electrodeposited on ITO at -1.15 V and 70°C for 2000 s in 0.1 M KNO₃ containing 10 mM Zn(NO₃)₂. As shown in the SEM image, the as-prepared ZnO sample exhibits uniformly grown and vertically aligned hexagonal structure with a diameter of $\sim 250\text{--}300 \text{ nm}$ and a length in the range of 700–800 nm. Figure 2A,B contains absorption spectra and diffuse reflectance data for as-deposited ZnO, showing the expected lack of significant optical absorption in the visible spectral range. The spectral cutoff (Figure 2A) at $\sim 400 \text{ nm}$ is consistent with this notion.

The band gap (E_g) of the ZnO nanowire array can be obtained from the diffuse reflectance data after performing the Kubelka–Munk transformation (Figure 2B) and using a Tauc plot^{28,29} (not shown). From such analyses, the value of E_g was estimated to be $\sim 3.4 \text{ eV}$, which is in good agreement with values reported in the literature for this oxide.¹ Photocurrent transients were also measured in the 0.1 M KNO₃ supporting electrolyte at a fixed bias potential of 0.50 V. Figure 1B shows that ZnO is an n-type semiconductor, as confirmed from the anodic polarity of the photocurrent.

XRD patterns and EDX spectra were obtained to characterize the composition of the electrodeposited ZnO nanowire array samples. Interestingly enough, diffraction patterns from metallic Zn were also observed along with peaks attributable to ZnO (Figure 3). In addition, EDX analysis reveals that the Zn to O

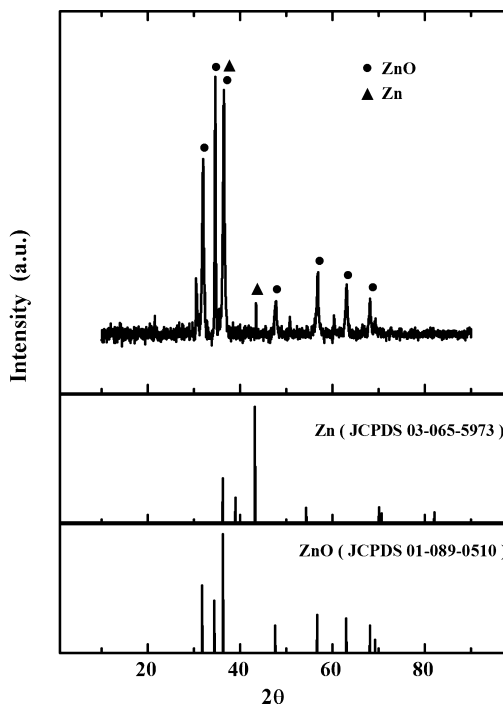


Figure 3. XRD pattern for Zn-ZnO nanorod array electrodeposited on ITO at -1.15 V in a 0.1 M KNO₃ electrolyte containing 10 mM Zn(NO₃)₂ for 2000 s.

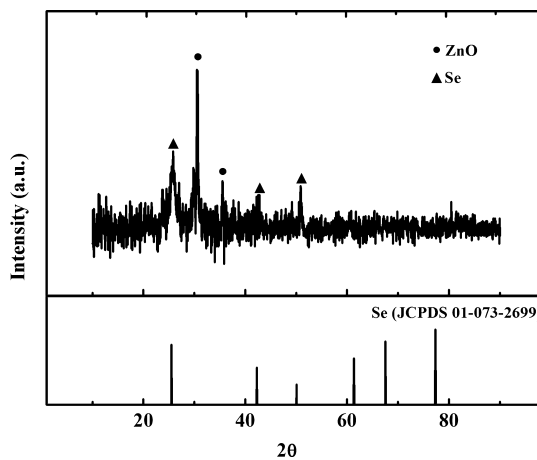


Figure 4. XRD pattern for a Se/ZnO composite electrode prepared by the galvanic replacement reaction. Zn/ZnO composite was first electrodeposited and then immersed in a 50 mM SeO₂ solution for 300 s.

ratio was substantially higher than unity, which implies the presence of metallic Zn codeposited with ZnO. The amount of metallic Zn decreased as the deposition potential and temperature were increased, as shown by EDX and XRD. Similar results have been recently reported by other research groups.^{30–32} For example, metallic Zn was observed during the electrochemical growth of ZnO nanobelts.³²

3.2. Conversion of Zn/ZnO Nanowire Array to Se/ZnO.

This excess metallic Zn, instead of being a nuisance, turns out to offer a fortuitous route for preparing Se/ZnO by galvanic displacement. Indeed, replacement of Zn with another metal, known as “zincation,” is a well-established technique in the electroplating community.³³ The idea in the present concept is

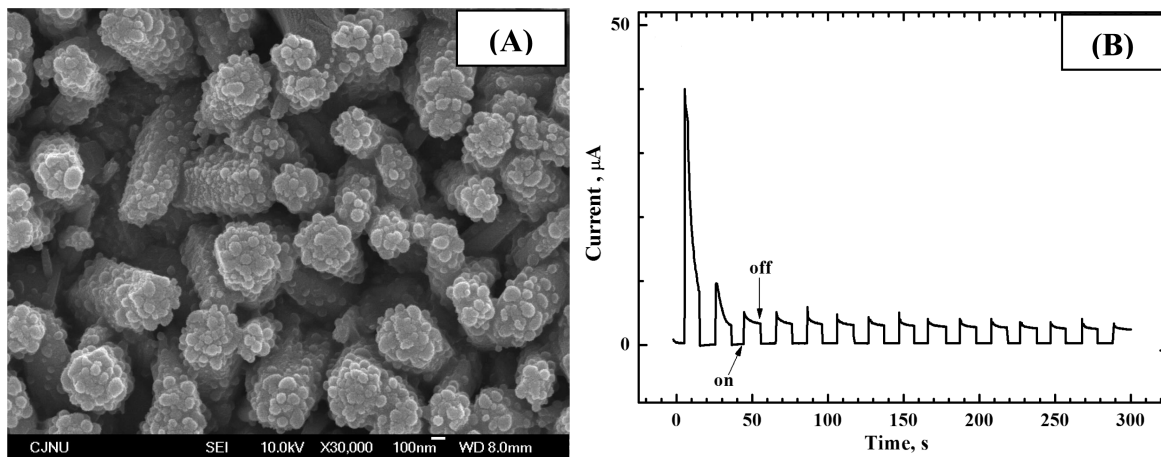


Figure 5. (A) SEM image of a Se/ZnO composite electrode prepared by the galvanic replacement reaction. Zn/ZnO composite was electrodeposited by the procedure in Figure 1A and immersed in a 50 mM SeO_2 solution for 300 s. (B) Photocurrent transients in 0.1 M KNO_3 supporting electrolyte at a fixed potential of -0.30 V for this sample.

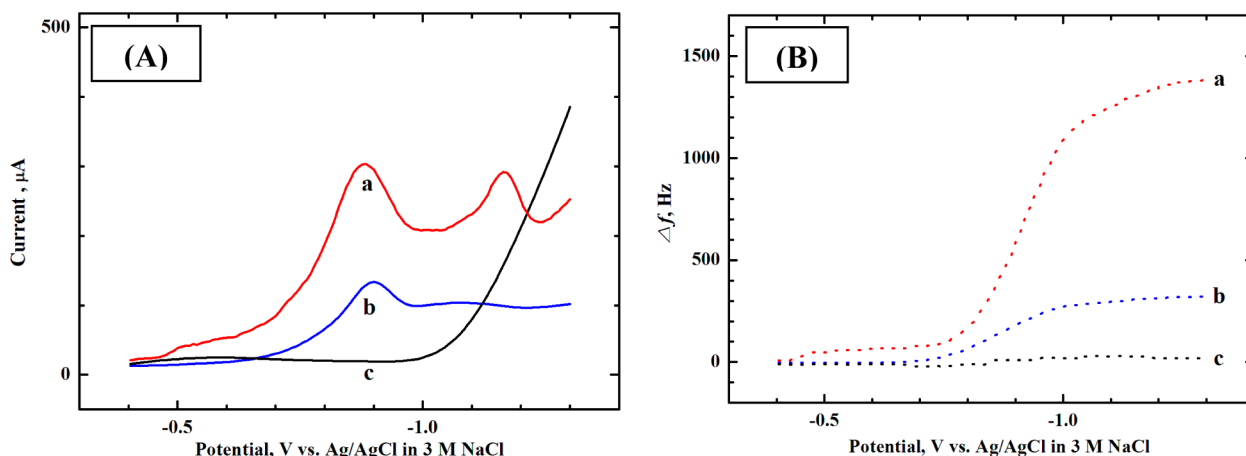
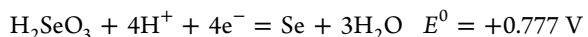
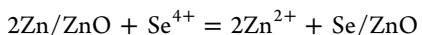


Figure 6. (A) Linear sweep voltammograms for ZnO electrodeposited on Au-quartz electrode at -1.15 (b) and -1.25 V (a,c) for 300 s using 0.1 M KNO_3 containing 10 mM $\text{Zn}(\text{NO}_3)_2$ at 70°C , followed by a galvanic replacement reaction in a 50 mM SeO_2 solution for 20 s at room temperature. Sample c was obtained after annealing at 250°C in air for 1 h. Voltammograms were obtained in a 0.1 M Na_2SO_4 electrolyte at a potential scan rate of 10 mV/s. (B) Corresponding EQCM frequency changes during the potential sweep in panel A.

to galvanically replace Zn with Se by placing the as-prepared Zn/ZnO nanowire array in a Se^{4+} containing bath



The redox potential gradient³⁴ is appreciable, as seen above, and serves to drive the galvanic displacement of Zn in the film with Se from the solution phase



To demonstrate this, we first prepared the ZnO nanowire array electrode as above. However, two different deposition potentials, that is, -1.15 and -1.25 V, were now employed to prepare ZnO electrodes with different amounts of metallic Zn. Their color gradually changed to red when placed in a 50 mM SeO_2 solution for 300 s. The color change was faster and deeper for the ZnO electrode electrodeposited at -1.25 V than the counterpart obtained at -1.15 V. This film appearance change is attributed to the Se component, which galvanically replaced the metallic Zn in ZnO. Concomitantly significant visible-light absorption occurred in the film (Figure 2A,B),

consistent with the much lower energy band gap of Se relative to ZnO. A Tauc plot (not shown) affords an E_g value for Se of ~ 1.9 eV, in good agreement with literature values for this semiconductor.³⁵

Figure 4 contains XRD data confirming the galvanic formation of Se on the parent ZnO surface. The Se phase is crystalline as deposited and appears as the rhombohedral modification.³⁶ There were no shifts of the XRD peaks for ZnO when Se was galvanically deposited on it, signaling that doping of the ZnO lattice with Se did not occur to any significant extent. This is not surprising considering the thermally mild conditions of the deposition in this study. Close examination of Figure 4 also reveals that diffraction peaks expected at higher angles ($\sim 60^\circ$) for Se are missing, perhaps symptomatic of particular crystallite orientation. Figure 5A contains SEM data showing the significant modification of the ZnO nanowire morphology when Se is deposited on its surface (c.f., Figures 1A and 5A). Despite surface alterations, however, the intrinsic original length and the 1-D nature of the nanowire array were maintained after the galvanic displacement step (Figure 5A). The diameter of the Se nanoparticles on the parent ZnO surface varies from 40 to 50 nm. Importantly, irradiation of Se/

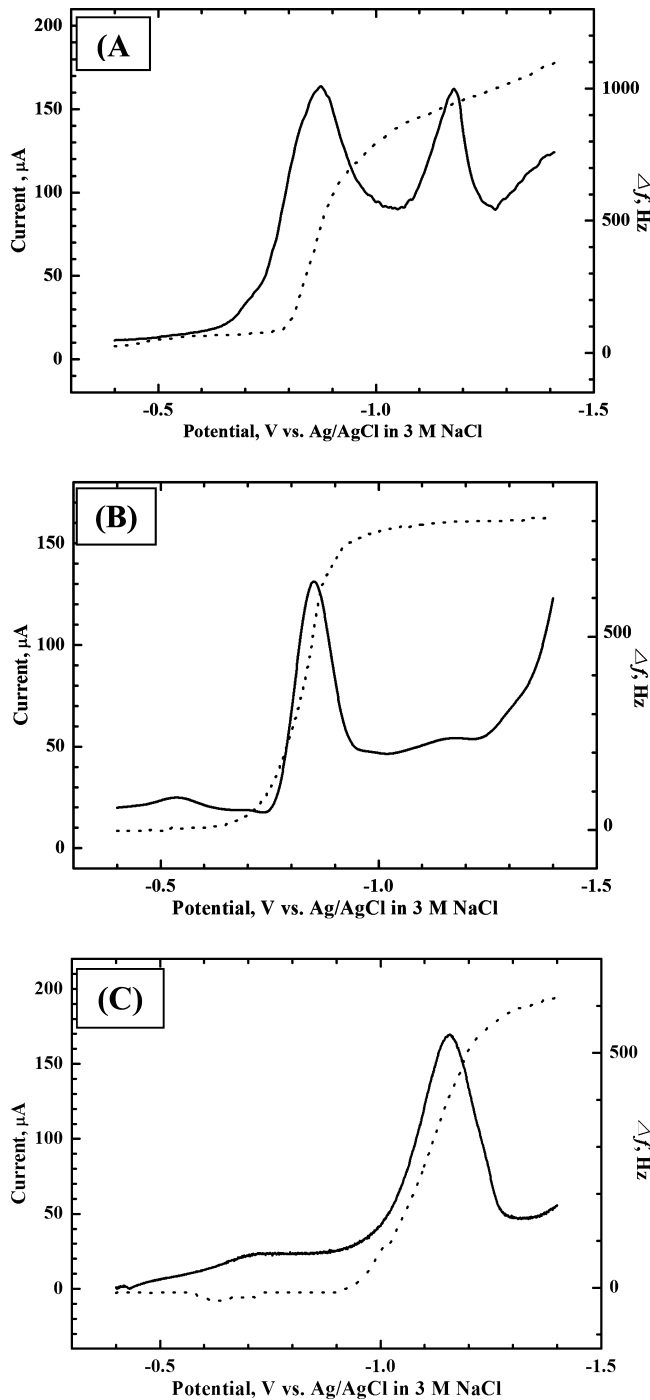


Figure 7. Linear sweep voltammograms (—) and corresponding frequency changes (----) for Au EQCM electrodes modified with (A) ZnSe thin film electrodeposited at -0.85 V for 200 s using a 0.1 M Na₂SO₄ electrolyte containing 2 mM SeO₂ and 0.1 M ZnSO₄, (B) Se thin film electrodeposited at -0.70 V for 200 s using 2 mM SeO₂ in 0.1 M Na₂SO₄ and (C) same electrode as in panel A but after complete removal of elemental Se by applying a potential of -0.85 V in a 0.1 M Na₂SO₄ blank electrolyte. Linear sweep voltammograms and corresponding frequency changes were obtained in 0.1 M Na₂SO₄ electrolyte at a potential scan rate of 10 mV/s.

ZnO generates *cathodic* photocurrents (Figure 5B), consistent with the p-type semiconductor nature³⁵ of the new Se phase.

To probe further the influence of the initial excess Zn component on Se/ZnO formation, we performed experiments

combining EQCM-linear sweep voltammetry. The results appear in Figure 6. First, ZnO was electrodeposited on the Au-quartz electrode at -1.15 and -1.25 V for 300 s using 0.1 M KNO₃ containing 10 mM Zn(NO₃)₂ at $70\text{ }^\circ\text{C}$. Deposition and concomitant mass increase can be monitored from the frequency decrease. After electrodeposition and thorough cleaning of the cell, the ZnO-coated Au-quartz electrode was placed in 50 mM SeO₂ solution for 20 s.

Linear sweep voltammetry reveals formation of Se/ZnO composite, as shown in Figure 6A. Voltammograms were obtained in 0.1 M Na₂SO₄ electrolyte with a scan rate of 10 mV/s. Voltammogram (a) in Figure 6A was obtained from the Se/ZnO composite, which was prepared at -1.25 V , followed by the galvanic displacement reaction. The first cathodic wave at -0.88 V is assigned to Se reduction (to Se²⁻),³⁷ and the second wave at $\sim-1.19\text{ V}$ is assigned to reduction of ZnSe to Zn and Se²⁻ (see below).¹⁶ Voltammogram (b) was obtained for the ZnO electrodeposited at -1.15 V , followed by the galvanic displacement. As described above, the content of metallic Zn in ZnO decreased with a deposition potential increase, and concomitantly the height of Se reduction wave also decreased. Notably, the peak at -1.19 V , assigned to ZnSe reduction, did not appear in voltammogram (b).

Dramatic change was observed after annealing the as-prepared ZnO electrode at $250\text{ }^\circ\text{C}$ in air for 1 h to convert metallic Zn to ZnO.⁴¹ Although ZnO was electrodeposited at -1.25 V and contained a substantial amount of metallic Zn, no peak from Se reduction was observed. This observation implies that the galvanic displacement reaction occurred only when metallic Zn was initially present in the film. Figure 6B shows the concomitant EQCM frequency increase (mass decrease) during the potential sweep. Taken together, the voltammetric and microgravimetric data in Figure 6 clearly show that the amount of metallic Zn is dependent on the electrodeposition potential, as expected.

To corroborate further the voltammogram assignments in Figure 6A, we electrodeposited a thin film of ZnSe¹⁸ on the Au electrode at -0.85 V for 200 s using a 0.1 M Na₂SO₄ electrolyte containing 2 mM SeO₂ and 0.1 M ZnSO₄. During a negative-going scan of this electrode in 0.1 M Na₂SO₄ blank electrolyte, two cathodic waves (and concomitant mass decrease) were observed (Figure 7A). Similarly, Se was electrodeposited on Au at -0.70 V for 200 s using 2 mM SeO₂ in 0.1 M Na₂SO₄.³⁶ Now, only one reduction wave was observed (Figure 7B). Finally, after electrodeposition of ZnSe at -0.85 V using a 0.1 M Na₂SO₄ electrolyte containing 2 mM SeO₂ and 0.1 M ZnSO₄, the free Se was completely stripped at -0.85 V in a 0.1 M Na₂SO₄ blank electrolyte. The resultant ZnSe film was further reduced, and only the cathodic wave at $\sim-1.18\text{ V}$ was observed with EQCM frequency increase (Figure 7C). These observations and the almost exact match of the voltammogram features in Figures 6 and 7 clearly support our assignment (see above) of the first wave to Se reduction and the second wave to ZnSe reduction. These data also demonstrate the viability of electrodeposition when combined with galvanic displacement for preparing Se/ZnO.

3.3. Conversion of Se/ZnO to CdSe/ZnO via Photocathodic Deposition. ZnO was first electrodeposited on the Au EQCM electrode at -1.15 V for 300 s using 0.1 M KNO₃ containing 10 mM Zn(NO₃)₂ at $70\text{ }^\circ\text{C}$, followed by a galvanic displacement in a 50 mM SeO₂ solution to produce Se/ZnO composite, as described in the preceding section. In the “dark”, neither frequency change nor current flow occurred when a

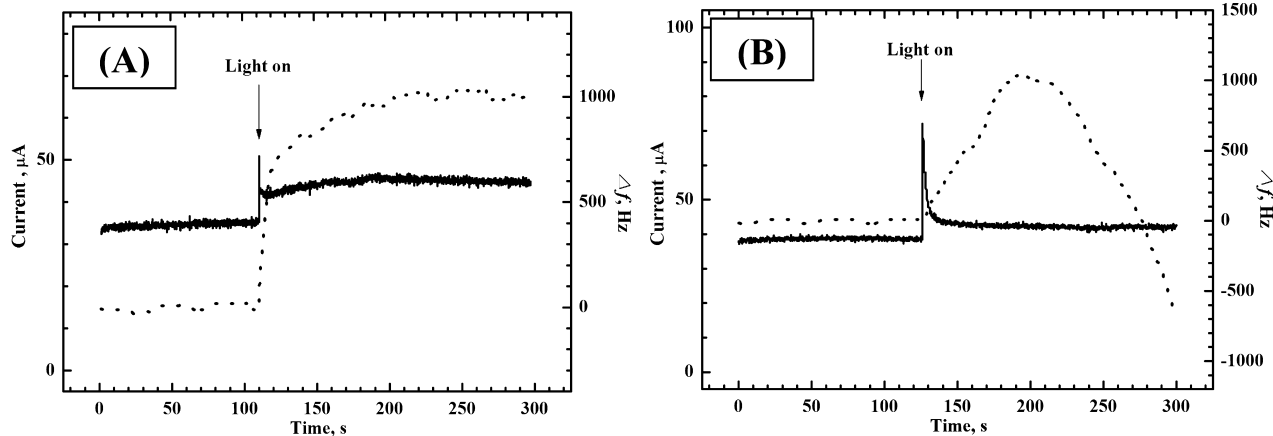


Figure 8. Current flow (—) and corresponding frequency change (----) in the dark and under illumination for (A) 0.1 M KNO₃ electrolyte and (B) same electrolyte also containing 20 mM CdSO₄ at the potential of -0.30 V. ZnO nanowire array electrodeposited on ITO at -1.15 V and 70 °C for 2000 s in 0.1 M KNO₃ electrolyte containing 10 mM Zn(NO₃)₂, followed by a galvanic replacement reaction in a 50 mM SeO₂ solution for 300 s to produce Se/ZnO.

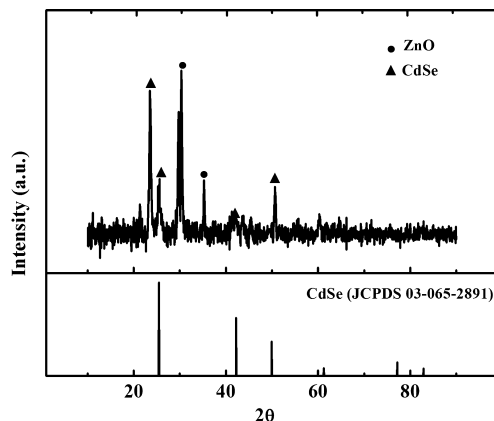


Figure 9. XRD pattern of a CdSe/ZnO composite sample synthesized, as described in Figure 8B.

potential of -0.30 V was applied to the Se/ZnO electrode in 0.1 M KNO₃ electrolyte. However, light illumination caused frequency increase as well as cathodic current flow, which is due

to the photocorrosion of Se to Se²⁻ species.^{35,39,40} After 300 s, all of the Se was stripped to Se²⁻, and no more frequency changes were seen (Figure 8A).

However, dramatic changes were observed when Cd²⁺ ions were added to the 0.1 M KNO₃ electrolyte. A mass increase (attributable to CdSe formation) was immediately seen (Figure 8B). Importantly, no changes in frequency and current were observed in 0.1 M KNO₃ containing 20 mM CdSO₄ when a potential of -0.30 V was applied to the Se/ZnO electrode under the dark condition. This is diagnostic of the fact that photodissolution of Se (to Se²⁻) is a prerequisite for CdSe formation. The mechanistic aspects of CdSe formation on an oxide semiconductor surface have been discussed elsewhere.²²

The photosynthesized CdSe/ZnO nanowire array composite was characterized by SEM, XRD, EDX, and PEC measurements. The XRD data in Figure 9 are consistent with the conversion of Se to CdSe (hexagonal wurtzite form, ref 38) on the ZnO surface (c.f., Figures 4 and 9). The SEM data (Figure 10A) show that the CdSe nanoparticles on the ZnO parent surface are somewhat larger than Se (c.f., Figure 5A) and are in

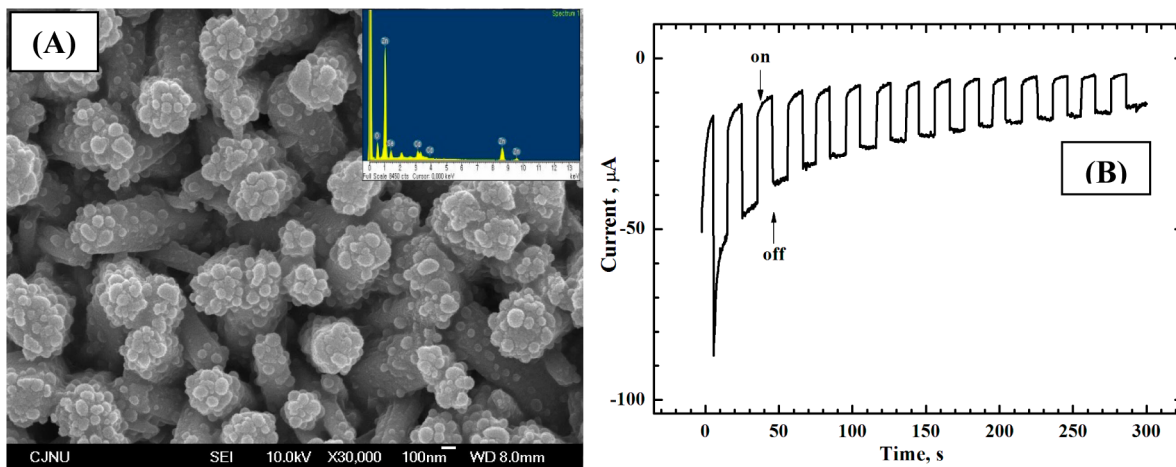


Figure 10. (A) SEM image of a CdSe/ZnO composite sample synthesized as described in Figure 8B. ZnO nanowire array electrodeposited on ITO at -1.15 V and 70 °C for 2000 s in 0.1 M KNO₃ electrolyte containing 10 mM Zn(NO₃)₂, followed by a galvanic replacement reaction in a 50 mM SeO₂ solution for 300 s to produce Se/ZnO. (B) Photocurrent transients in 0.1 M KNO₃ supporting electrolyte for this sample at a fixed potential of 0.40 V.

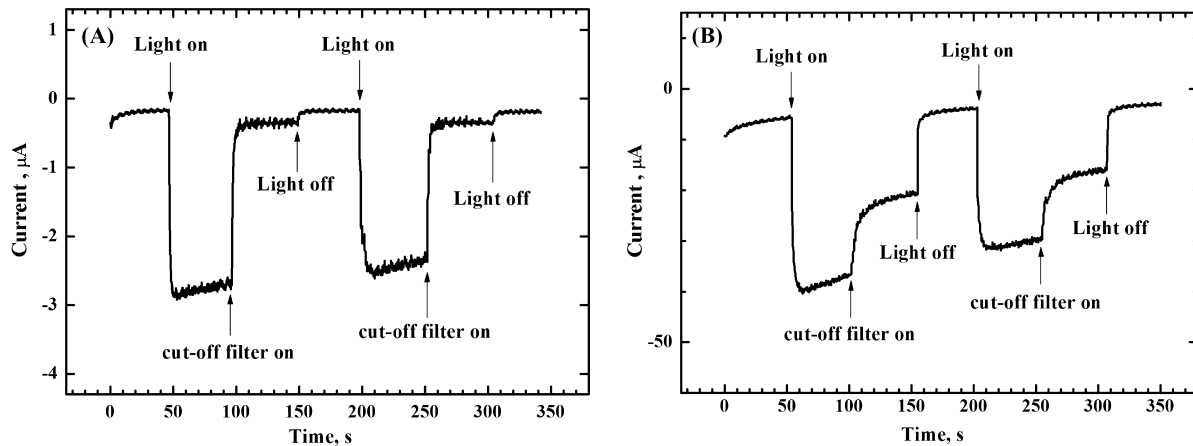


Figure 11. Photocurrent transients for a ZnO nanorod array (A) and CdSe/ZnO composite sample (B) in 0.1 M KNO_3 supporting electrolyte at a fixed potential of 0.40 V. ZnO and CdSe/ZnO were prepared as discussed in the text.

the ~ 50 – 60 nm diameter range. The EDX results (Figure 10A, insert) reveal the presence of both Se and Cd consistent with CdSe formation on ZnO. Quantitative analyses yielded an excess of Se relative to Cd (4.83 vs 3.46 atom %). This stoichiometric trend pervades in the cathodic deposition of CdSe,^{14–16} and we have previously shown how this excess Se can be readily removed via stripping voltammetry.⁴⁰

Diffuse reflectance spectroscopy (Figure 2A,B) show a spectral shift in the absorption cutoff consistent with the higher E_g of CdSe (~ 2.3 eV) relative to Se (~ 1.9 eV) (Figure 2B). As with Se/ZnO, CdSe/ZnO also exhibits significant absorption in the visible range, attesting to the effectiveness of spectral sensitization of ZnO with CdSe. The photocurrent at 0.40 V in the 0.1 M KNO_3 electrolyte is now anodic; diagnosing that p-Se had been converted to n-type CdSe on the parent ZnO surface (Figure 10B).

Finally Figure 11 compares photocurrent transients for the parent ZnO nanowire array (Figure 11A) contrasted with those for CdSe/ZnO (Figure 11B). When the cutoff filter is inserted, the photocurrent immediately dies down, consistent with the lack of visible light response of ZnO (Figure 11A). On the other hand, an “extra” photocurrent component in the visible-light regime is clearly seen in the transients for the CdSe/ZnO case (Figure 11B).

4. CONCLUDING REMARKS

A facile method for the preparation of Se/ZnO and CdSe/ZnO nanowire arrays has been presented above. This hybrid scheme uses a combination of electrodeposition of ZnO, galvanic displacement of the excess Zn (in ZnO) with Se, and photoinduced reduction of Se to Se^{2-} in a Cd^{2+} -containing electrolyte to produce CdSe nanoparticles on the parent ZnO nanowire surface. The excess Zn that is a perennial problem in electrodeposited ZnO films^{16,27,29} has been utilized as a sacrificial reductant in this approach. The amount of excess Zn (and thus, ultimately, CdSe) was found to scale with the electrodeposition potential. It is worth noting that the scheme developed in this study is completely general and should be applicable to other composite semiconductor systems as long as the solution precursor species are capable of galvanically displacing one of the initially electrodeposited film components. The component thus deposited should also undergo cathodic photocorrosion (i.e., stripping) in the second step and

simultaneously react with a metal ion in situ to form the second component of the composite in the final step of the sequence.

■ AUTHOR INFORMATION

Corresponding Author

*Tel: 817 272 5421. E-mail: myung@kku.ac.kr (N.M.) and rajeshwar@uta.edu (K.R.).

Present Address

[§] MEMC Korea Company, Cheonan, Chungnam 331-831, Republic of Korea.

Notes

The authors declare no competing financial interest.

■ ACKNOWLEDGMENTS

This research was supported by Basic Science Research Program through the National Research Foundation of Korea (NRF) funded by the Ministry of Education, Science and Technology (2009-0074367). The two anonymous reviewers are thanked for their constructive criticism of a previous manuscript version, and one of them is additionally thanked for alerting us to ref 25.

■ REFERENCES

- (1) For example: Kim, Y.-I.; Seshadri, R. *Inorg. Chem.* **2008**, *47*, 8437. See also references therein.
- (2) Tena-Zaera, R.; Elias, J.; Levy-Clement, C. *Appl. Phys. Lett.* **2008**, *93*, 233119.
- (3) Elias, J.; Tena-Zaera, R.; Wang, G.-Y.; Levy-Clement, C. *Chem. Mater.* **2008**, *20*, 6633.
- (4) Tang, Y.; Hu, X.; Chen, M.; Luo, L.; Li, B.; Zhang, L. *Electrochim. Acta* **2009**, *54*, 2742.
- (5) Chen, J.; Li, C.; Zhao, D. W.; Lei, W.; Zhang, Y.; Cole, M. T.; Chu, D. P.; Wang, B. P.; Cui, Y. P.; Sun, X. W.; Milne, W. I. *Electrochim. Commun.* **2010**, *12*, 1432.
- (6) Luan, C.; Vaneski, A.; Susha, A. S.; Xu, X.; Wang, H.-E.; Chen, X.; Xu, J.; Zhang, W.; Lee, C.-S.; Rogach, A. L.; Zaprien, J. A. *Nanoscale Res. Lett.* **2011**, *6*, 340.
- (7) Hodes, G. *J. Phys. Chem. C* **2008**, *112*, 17778.
- (8) Shen, Q.; Zhao, X.; Zhou, S.; Hou, W.; Zhu, J.-J. *J. Phys. Chem. C* **2011**, *115*, 17958.
- (9) Lim, C.-S.; Chen, M.-L.; Oh, W.-C. *Bull. Korean Chem. Soc.* **2011**, *32*, 1657.
- (10) Barpuzary, D.; Khan, Z.; Vinothkumar, N.; De, M.; Qureshi, M. *J. Phys. Chem. C* **2012**, *116*, 150.

- (11) Levy-Clement, C.; Elias, J.; Tena-Zaera, R. *Phys. Status. Solidi C* **2009**, *6*, 1596.
- (12) Majidi, H.; Baxter, J. B. *Electrochim. Acta* **2011**, *56*, 2703.
- (13) Tena-Zaera, R.; Katty, A.; Bastide, S.; Levy-Clement, C. *Chem. Mater.* **1626**, *2007*, 19.
- (14) Rajeshwar, K. *Adv. Mater.* **1992**, *4*, 23.
- (15) Hodes, G. In *Physical Electrochemistry*, Vol. 487; Marcel Dekker: New York, 1995, p 40.
- (16) Schlesinger, T. E.; Rajeshwar, K.; de Tacconi, N. R. Ch. 14. In *Modern Electroplating*; Schlesinger, M., Paunovi, M., Eds.; John Wiley & Sons: New York, 2010; p 383.
- (17) Sun, Y.; Xia, Y. *Science* **2002**, *298*, 2176.
- (18) Magagnin, L.; Bertani, V.; Cavallotti, P. L.; Maboudian, R.; Carraro, C. *Microelectron. Eng.* **2002**, *64*, 479.
- (19) Johnson, M.; Kelly, J. A.; Henderson, E. J.; Veinot, J. G. C. *IOP Conf. Ser.: Mater. Sci. Eng.* **2009**, *6*, 012031.
- (20) Mohl, M.; Dobo, D.; Kukovecz, A.; Konya, Z.; Kprdas, K.; Wei, J.; Vajtai, R.; Ajayan, P. M. *J. Phys. Chem. C* **2011**, *115*, 9403.
- (21) Chenthamarakshan, C. R.; Ming, Y.; Rajeshwar, K. *Chem. Mater.* **2000**, *12*, 3538.
- (22) Somasundaram, S.; Chenthamarakshan, C. R.; de Tacconi, N. R.; Ming, Y.; Rajeshwar, K. *Chem. Mater.* **2004**, *16*, 3846.
- (23) Levy-Clement, C.; Tena-Zaera, R.; Ryan, M. A.; Katty, A.; Hodes, G. *Adv. Mater.* **2005**, *17*, 1512.
- (24) Janaky, C.; de Taconni, N. R.; Chanmanee, W.; Rajeshwar, K. *J. Phys. Chem. C* **2012**, in press.
- (25) Dloczik, L.; Könenkamp, R. *Nano Lett.* **2003**, *3*, 651.
- (26) Zhang, L.; Chen, Z.; Tang, Y.; Jia, Z. *Thin Solid Films* **2005**, *492*, 24.
- (27) Ham, S.; Jeon, S.; Lee, U.; Park, M.; Paeng, K.-J.; Myung, N.; Rajeshwar, K. *Anal. Chem.* **2008**, *80*, 6724.
- (28) Finlayson, A. P.; Tsaneva, V. N.; Lyons, L.; Clark, M.; Glowacki, B. A. *Phys. Status Solidi A* **2006**, *203*, 327.
- (29) Pankove, J. L. *Optical Processes in Semiconductors*; Prentice Hall: Englewood Cliffs, NJ, 1971.
- (30) Hu, F.; Chan, K. C.; Yue, T. M.; Surya, C. *J. Phys. Chem. C* **2010**, *114*, 5811.
- (31) Wang, J.-G.; Tian, M.-L.; Kumar, N.; Mallouk, T. *Nano Lett.* **2005**, *5*, 1247.
- (32) Pradhan, D.; Su, S.; Sindhwan, S.; Honek, J. F.; Leung, K. T. *J. Phys. Chem. C* **2011**, *115*, 18149.
- (33) Schlesinger, M. Ch. 14. In *Modern Electroplating*; Schlesinger, M., Paunovi, M., Eds.; John Wiley & Sons: New York, 2010; p 131.
- (34) Bard, A. J.; Parsons, R.; Jordan, J. *Standard Potentials in Aqueous Solution*; Marcel Dekker: New York, 1985.
- (35) For example: Frese, K. W. *Appl. Phys. Lett.* **1982**, *40*, 275.
- (36) Miyamoto, Y. *Jpn. J. Appl. Phys.* **1980**, *19*, 1813.
- (37) Zhang, Y.; Wang, Y.; Deng, Y.; Li, M.; Bai, J. *ACS Appl. Mater. Interfaces* **2012**, *4*, 65.
- (38) Wei, C.; Rajeshwar, K. *J. Electroanal. Chem.* **1994**, *375*, 109.
- (39) Ham, S.; Choi, S.; Chae, Y.; Lee, W. J.; Paeng, K.-J.; Kim, W.-G.; Myung, N. *Bull. Korean Chem. Soc.* **2010**, *31*, 3403.
- (40) Ham, S.; Choi, B.; Paeng, K.-J.; Myung, N.; Rajeshwar, K. *Electrochim. Commun.* **2007**, *9*, 1293.
- (41) Sowa, H. *Solid State Sci.* **2005**, *7*, 1384.